Soft Matter

PAPER

View Article Online
View Journal | View Issue

Cite this: *Soft Matter*, 2020, **16**, 8057

Preoperative vascular surgery model using a single polymer tough hydrogel with controllable elastic moduli†

William C. Ballance,[a] Vignesh Karthikeyan,[a] Inkyu Oh,[b] Ellen C. Qin,[c] Yongbeom Seo,[a] Tremaan Spearman-White,[d] Rashid Bashir,[def] Yuhang Hu,[g] Heidi Phillips[h] and Hyunjoon Kong*[aefi]

Received 26th May 2020,
Accepted 7th August 2020

DOI: 10.1039/d0sm00981d

rsc.li/soft-matter-journal

Materials used in organ mimics for medial simulation and education require tissue-like softness, toughness, and hydration to give clinicians and students accurate tactile feedback. However, there is a lack of materials that satisfy these requirements. Herein, we demonstrate that a stretchable and tough polyacrylamide hydrogel is useful to build organ mimics that match softness, crack growth resistance, and interstitial water of real organs. Varying the acrylamide concentration between 29 or 62% w/w with a molar ratio between cross-linker and acrylamide of 1 : 10 800 resulted in a fracture energy around ~2000 J m^{-2}. More interestingly, this tough gel permitted variation of the elastic modulus from 8 to 62 kPa, which matches the softness of brain to vascular and muscle tissue. According to the rheological frequency sweep, the tough polyacrylamide hydrogels had a greatly decreased number of flow units, indicating that when deformed, stress was dispersed over a greater area. We propose that such molecular dissipation results from the increased number of entangled polymers between distant covalent cross-links. The gel was able to undergo various manipulations including stretching, puncture, delivery through a syringe tip, and suturing, thus enabling the use of the gel as a blood vessel model for microsurgery simulation.

Introduction

Complex surgeries performed on organs of various kinds require careful preoperative planning and extensive training to develop the necessary muscle memory and spatial understanding required to successfully treat patients. Due to emerging simulation tools, such as 3-D printing, there has been a growing interest in assembling organ mimics for surgical training and preoperative surgical planning.[1,2] However, the materials commonly used for such applications are often silicone or polymer-based elastomers. These materials have stiffness many times that of real human organs and do not include the interstitial water contained in native organs.[3] Such models would give surgeons an inappropriate idea of the magnitude of force required to perform many operations and lack the tactile feel of interstitial tissue fluid. In addition, such materials often lack mechanical toughness and cannot be used to create incisions or place sutures without extensive crack propagation. Also, researchers have used cryopreserved organs for surgery simulation, but these have limited supply due to the need for human or animal donors and have altered physical properties after cryopreservation.[4] As such, hydrogels with softness and interstitial media have garnered attention as an alternative synthetic building material that can potentially alleviate these limitations.[5–8] Unfortunately, hydrogels commonly exhibit limited utility in environments and applications where large shear forces and deformations are present due to their intrinsic brittleness.

[a] *Department of Chemical and Biomolecular Engineering, University of Illinois at Urbana-Champaign, Urbana, IL 61801, USA. E-mail: hjkong06@illinois.edu; Fax: +1 217 333 5052*
[b] *Department of Mechanical Science and Engineering, University of Illinois at Urbana-Champaign, Urbana, IL 61801, USA*
[c] *Department of Materials Science and Engineering, University of Illinois at Urbana-Champaign, Urbana, IL 61801, USA*
[d] *Department of Bioengineering, University of Illinois at Urbana-Champaign, Urbana, IL 61801, USA*
[e] *Beckman Institute for Advanced Science and Technology, University of Illinois at Urbana-Champaign, Urbana, IL 61801, USA*
[f] *Carl R. Woese Institute for Genomic Biology University of Illinois at Urbana-Champaign, Urbana, IL 61801, USA*
[g] *The George W. Woodruff School of Mechanical Engineering, Georgia Institute of Technology, Atlanta, GA 30332, USA*
[h] *College of Veterinary Medicine, University of Illinois at Urbana-Champaign, Urbana, IL 61801, USA*
[i] *Department of Medical Engineering, Yonsei University, College of Medicine, Seoul, 03722, Republic of Korea*

† Electronic supplementary information (ESI) available. See DOI: 10.1039/d0sm00981d

The limited deformability of hydrogels stems from their microstructure: the material is composed of $>90\%$ water, with a relatively small concentration of polymer stabilizing the overall structure. As a result, hydrogels have a limited capability to dissipate energy within their structure and can only withstand a limited degree of strain before fracture.[9] Additionally, there is an intrinsic trade-off in these cross-linked networks between fracture toughness and stiffness.[10,11] Namely, increasing the cross-linking density within a hydrogel leads to a matrix with increased stiffness and decreased toughness and stretchability.

To alleviate this weakness, many researchers have developed tough and stretchable hydrogels by engineering reversible, non-covalent interactions between gel-forming polymers.[12] For example, adding a sacrificial interpenetrating network of secondary polymer within a base hydrogel reinforces the toughness of the gel; as the gel is stretched, the secondary network can dissipate energy by fracturing while the base network remains intact.[13] Other strategies to form more fracture-resistant hydrogels involve the introduction of functional groups that form ionic or electrostatic bonds to the gel-forming polymers. These reversible bonds allow for dissipation of work throughout the gel as it is stretched while an elastic covalent network stabilizes the overall material.[14] Another form of tough gels are topological hydrogels.[15] These gels contain non-chemical bonds that are created by physically impeding the mobility of a part of the polymer. For example, such a gel may be formed by threading polyethylene glycol chains through α-cyclodextrin rings.[16] When stretched, the cyclodextrin rings can dissipate energy by sliding down the polyethylene glycol chains. These recently developed tough hydrogels have been utilized to engineer resilient cartilage replacements, soft actuators, and flexible electronics.[17–19] However, these binary gel systems have never been used to assemble 3D organ mimics crucial for preoperative surgical planning and simulation. In fact, many of these hydrogels are complicated in their synthesis and microstructure, which impedes their translation into engineering material contexts. In addition, it is challenging to control the elastic modulus of the gel and, in turn, reproduce tissue-like softness while keeping high stretchability and toughness. In general, the gel becomes brittle when the gel is too soft or stiff.

In this study, we hypothesize that a one-component, elastic, tough, and stretchable hydrogel would be engineered without the need for secondary polymers and functional groups by increasing gel-forming polymer concentration and decreasing the number of covalent cross-links. As the polymeric length between cross-links play a major role in dissipating energy for fracture, it would be possible to control an elastic modulus with minimal change of toughness by tuning the ratio between gel-forming polymer concentration and a cross-linking ratio.[20–22] Due to superior resistance to fracture, the one-component stretchable hydrogel would also allow for various manipulations such as twisting, bending, punctuation, and suturing.

We examined this hypothesis by using polyacrylamide as a model gel-forming polymer. This polymer was chosen because polyacrylamide exhibits a potential to form transient interactions between polymer chains including physical entanglements and hydrogen bonding.[23] In addition, polyacrylamide has been used extensively as the elastic component in multi-component stretchable gels.[24,25] The single-component, elastic, tough and stretchable hydrogels were assembled by varying overall acrylamide concentration from 29 to 62% g acrylamide per g total gel (w/w) while using a low molar ratio of bis-acrylamide: acrylamide, denoted as the cross-linker ratio, of 1 : 10 800. These gels were then evaluated for the elastic modulus and the response in fracture energy to tensile strain rate and dynamic mechanical behavior, including hysteresis and rheological characterization. Finally, we examined the extent that the one-component elastic, tough and stretchable gel can deform its shape reversibly in response to various mechanical perturbations common to surgical handling and also allow for manipulation such as puncturing, suturing, and needle-based injection relevant to a high-fidelity surgical planning and simulation tool.

Results

1. Analysis of hydrogel fracture

First, we characterized the tensile mechanical properties of a gel by stretching the pre-swollen gel strip uniaxially until fracture. A brittle polyacrylamide gel was prepared with a cross-linker ratio (mol methylene bis-acrylamide : mol acrylamide) of 1 : 63 and acrylamide concentration of 9% w/w (g acrylamide per total weight of solution) (Fig. 1a–i). The gel fractured before it was extended to twice of its original length. In contrast, the hydrogels prepared at a cross-linker ratio of 1 : 10 800 while varying acrylamide concentration of the pre-gelled solution from 29 to 44, 55, and 62% w/w could be stretched more than three times than the brittle gel. In particular, the gel prepared with 29% w/w acrylamide solution was stretched up to 1300% of its original length (Fig. 1a-ii and Fig. S.1, ESI†). Further increase of the acrylamide concentration to 62% decreased the ultimate tensile strain to 570%. This ultimate strain is still more than three-fold higher than the brittle gel prepared with 9% w/w acrylamide solution and a cross-linker ratio of 1 : 63.

The tensile elastic modulus of the stretchable gels quantified with the first 10% of stress *versus* strain curve was increased with acrylamide concentration in a linear manner (Fig. 1b). Thus, the tensile elastic moduli of the gels ranged from 6.3 ± 0.2 to 64.3 ± 8.5 kPa for gels with an acrylamide concentration of 26 to 62% w/w. In addition, the volume fraction of polymer in the hydrogels was calculated from the dry and swollen mass of the hydrogels. The volume fraction of polymer of the gels increased from 0.039 ± 0.001 to 0.094 ± 0.001 m^3 m^{-3} as the acrylamide concentration increased from 29 to 62% w/w at a cross-linking ratio of 1 : 10 800. The brittle gel prepared with 9% w/w acrylamide solution and a cross-linker ratio of 1 : 63 had a volume fraction of polymer of 0.049 ± 0.002 m^3 m^{-3} (Fig. S.2, ESI†).

The number of elastically effective cross-links per volume of the gel ($N_{\text{cross-link}}$) at swelling equilibrium was calculated from rubber elasticity using the measured shear modulus (G) at

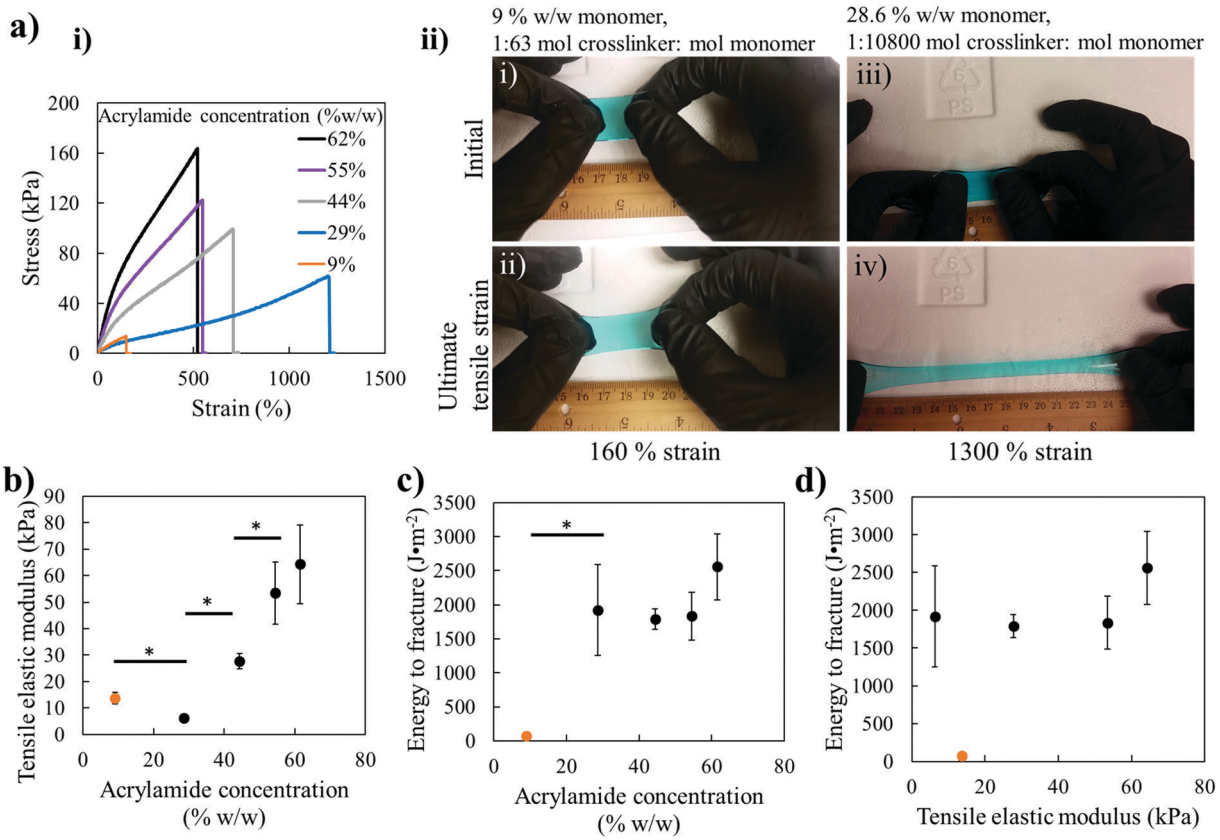

Fig. 1 Tensile mechanical properties of hydrogels (a) Tensile tests were performed on hydrogels prepared with various concentrations of acrylamide and a molar cross-linker ratio of 1 : 10 800 until fracture. The strain rate was kept constant at 0.1 s^{-1}. A brittle gel (depicted in the orange line and point) prepared by cross-linking 9%w/w acrylamide solution at 1 : 63 was used as a control. The data depicted are (i) the stress *vs.* strain curves and photographs of hydrogels when manually stretched until fracture. The stress *vs.* strain curves were analyzed to obtain (b) elastic modulus and (c) the energy to fracture. (d) The relationship between elastic modulus and energy to fracture for gels with acrylamide concentrations of 29%, 44%, 55%, and 62%. All samples are formed with a molar cross-linker ratio of 1 : 10 800. The values and error bars represent average and standard deviation of three different samples per condition. * indicates statistically significant difference in the means between samples according to a *T*-test with $p < 0.05$. Orange points and lines depict samples formed with a cross-linker ratio (mol methylene bis-acrylamide to mol acrylamide) of 1 : 63. All other samples are formed with a molar cross-linking ratio of 1 : 10 800.

volume fraction of polymer (ν_p) at swelling equilibrium.[26] $N_{cross\text{-}link}$ significantly increased from 2.6 to 23.6 mol m^{-3} with increasing acrylamide concentration from 29 to 62% w/w (Table 1). Effective cross-links denote both chemical covalent cross-links and polymer chain entanglements. If the gels were solely cross-linked through covalent bounds, after equilibrium swelling in water the gels should reach the same number of cross-links per volume, since the molar cross-linker ratio was not changed.

Table 1 Measurement of polymer volume fraction in swollen gel and rubber elasticity prediction of number of cross-links of gels

Concentration (w/w) (g g^{-1})	Cross-linker ratio (bis-acrylamide : acrylamide)	Polymer volume fraction (ν_p) m^3 m^{-3}	Effective number of cross-links (N) mol m^{-3}
9%	1 : 63	0.049	2.8
29%	1 : 10 800	0.039	2.6
44%	1 : 10 800	0.068	7.9
55%	1 : 10 800	0.080	13.0
62%	1 : 10 800	0.094	23.6

However, this was not the case indicating the effective number of cross-links includes entanglement interactions. This finding demonstrates that the increase in gel elastic modulus was related to the density of entanglements in the gel, which increased with overall concentration.

Next, the energy absorbed up to the point of fracture was quantified with an area under the force *versus* extension curves and normalized by the cross-sectional area of the gel sample. Hydrogels prepared with 29 to 55% w/w acrylamide solution exhibited an average fracture energy around 1850 J m^{-2}, despite the decrease of the ultimate strain (Fig. 1c). The gel prepared with 62% w/w acrylamide solution showed a further increased energy of 2560 J m^{-2}. The fracture energy of the brittle gel prepared with 9% w/w acrylamide solution was 68 J m^{-2}. Overall, the 29 to 55%w/w polyacrylamide gels prepared herein displayed an increase in both the elastic modulus and the fracture energy (Fig. 1d).

Next, we examined extent that the tough and stretchable gel resists fracture propagation by introducing notches of varied length into hydrogel strips before uniaxial stretching (Fig. 2a).

This analysis would allow us to address the mechanism by which acrylamide concentration serves to increase the fracture energy.[27,28] Interestingly, the dependency of the energy to fracture on the distance between notches became larger with increasing concentration of the acrylamide (Fig. 2b). However, the hydrogel made with 9% w/w acrylamide and a molar cross-linker ratio of 1 : 63 showed a decrease in energy to fracture of more than an order of magnitude.

The work dissipated outside the fracture process zone (w_0) was approximated using the slope of the dependency of the distance between notches and energy to fracture for all the samples (Fig. S.3, ESI†).[10,29,30] The fracture process zone is defined as the area in the leading edge of the propagating crack in which fracture occurs. w_0 for each of the samples was normalized by w_0 of the hydrogel made with 9% w/w acrylamide and a molar cross-linker ratio of 1 : 63 (Fig. 2c). Accordingly, the normalized w_0 increased with acrylamide concentration, regardless of the cross-linking ratio. In particular, the 62%w/w gel that exhibited the highest fracture energy in the Fig. 1 showed 34-fold higher w_0 than the 9%w/w gel exhibiting the smallest fracture energy. Likewise, the 29% w/w gel exhibiting the highest ultimate tensile strain displayed an 8-fold increase in the w_0 compared to the 9%w/w gel exhibiting the smallest fracture energy. In contrast, the contribution of w_p to the gel fracture energy was negligible (Fig. S.4, ESI†).

2. Analysis of rate-dependent dissipation

Increases in w_0 of the gels were further related to the gel's ability to reduce the dependency of the energy absorbed up to fracture on the strain rate (Fig. 3a). The ability of a gel to dissipate energy depends on transient, interactions between entangled polymers which have a characteristic timescale over which they act. Therefore, strain rates that are faster than the relaxation rate of the gel result in an earlier onset of fracture. The tensile elastic modulus was largely unaffected by the strain rate, regardless of the concentration of acrylamide of the gel (Fig. 3b). This is likely because the gel behaves like an elastic solid during the initial tensile deformation. However, as the material was elongated higher than 10% of original length, the strain rate became important, particularly for tough and stretchable gels, as quantified by the ultimate strain and fracture energy (Fig. 3c and d). The stretchable hydrogels prepared with the 29 and 62% w/w acrylamide solution exhibited large dependencies of the ultimate strain and the fracture energy on the strain rate. In contrast, the ultimate strain and the fracture energy of the brittle gel prepared with 9% w/w acrylamide solution were independent of the strain rate.

We further modified the stress *versus* strain curves of the hydrogels shown in Fig. 3a to the true stress *versus* $\lambda^2 - 1/\lambda$ where true stress is uniaxial force divided by the cross-sectional area assuming the material is incompressible and λ is the extension ratio (*i.e.*, stretched length divided by original length).[31] The resulting linear behavior in Fig. S.5 (ESI†) supports the use of rubber elasticity to describe the hydrogel mechanical behavior.

3. Analysis of the strength and number of flow units of hydrogels

We analyzed viscoelastic response of the gel by imposing an oscillatory shear on the gel at varied frequencies within a linear elastic region. This analysis allows us to quantitatively examine the dynamic mechanical behavior of the gel (Fig. 4a and Fig. S.6, ESI†). Interestingly, tough gels with an energy to fracture larger than 1000 J m^{-2} exhibited the larger dependency of the elastic modulus on frequency. In particular, the dependency became larger with increasing acrylamide concentration from 29 to 62% at a cross-linker ratio of 1 : 10 800. In contrast, the brittle gel prepared with 9% acrylamide solution at a cross-linker ratio of 1 : 63 displayed an independency of the storage modulus on frequency. The loss factor (*i.e.*, the ratio of loss to elastic modulus) was also quantified from the frequency sweep tests (Fig. S.7, ESI†). All the gels showed loss factors lying around 0.1,

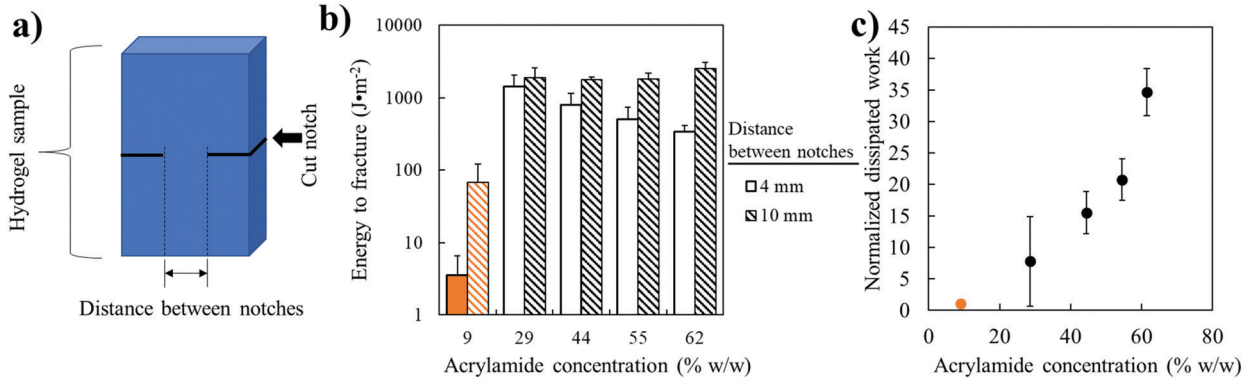

Fig. 2 Calculation of dissipated work from tensile tests on hydrogels with varied notch length (a) Tensile tests were performed after cutting notches with distance between of notches of 4 mm as well as without notches, as depicted by the schematic. (b) The fracture energy values were used to calculate (c) the work dissipated outside of the fracture process zone for gels of various concentrations which was normalized by the work dissipated in the gel formed with 9% w/w acrylamide and a molar cross-linker ratio of 1 : 63. The values and error bars represent average and standard deviation of three different samples per condition. * indicates statistically significant difference in the means between samples according to a *T*-test with $p < 0.05$. Orange points and bars depict samples formed with a cross-linker ratio of 1 : 63. All other samples are formed with a molar cross-linking ratio of 1 : 10 800.

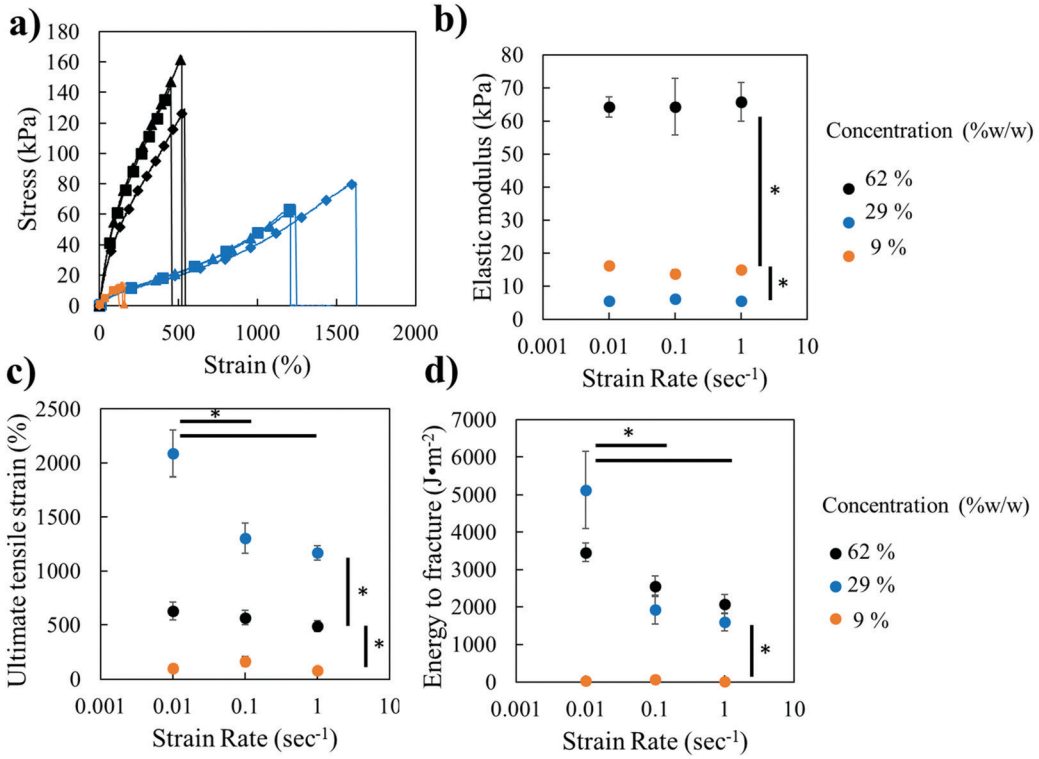

Fig. 3 Strain rate-dependent tensile mechanical properties of hydrogels Tensile tests at varied strain rates were performed on hydrogels with 29% and 62% w/w concentration of acrylamide at a cross-linking ratio of 1 : 10 800 as well as hydrogels with 9% w/w concentration of acrylamide at a cross-linking ratio of 1 : 63. The data depicted are (a) the stress *vs.* strain curves for the samples at 3 different formulations, (b) modulus, (c) strain at break, and (d) the energy absorbed until fracture. The values and error bars represent average and standard error of at least five different samples per condition. * indicates statistically significant difference in the means between samples according to a *T*-test with $p < 0.05$. Vertical statistical significance lines refer to differences between sample formulation whereas horizontal lines refer to difference between the same sample formulation taken at a difference strain rate. Orange lines and points depict samples formed with a cross-linking ratio of 1 : 63. All other samples are formed with a cross-linking ratio of 1 : 10 800. Diamonds (♦) indicate samples strained at a rate of 0.01 s^{-1}, triangles (▲) indicate a strain rate of 0.1 s^{-1}, and squares (■) indicate a strain rate of 1 s^{-1}.

which are higher than a loss factor of the brittle hydrogel with the 9% w/w/acrylamide and the cross-linker ratio of 1 : 63.

The data points collected from the oscillatory shear test was further fitted to a dissipative flow unit gel model, in order to quantify the gel strength and the number of flow units (*i.e.*, solid black line in Fig. 4a).[32] This model can be expressed as eqn (1):[33,34]

$$G^*(\omega) = \sqrt{G'(\omega)^2 + G''(\omega)^2} = A_F \omega^{1/z} \quad (1)$$

where G^*, G', and G'' are the complex, storage, and loss moduli; ω is the oscillation frequency; A_F is the gel strength, and z is the number of flow units. The number of flow units indicate each group of polymer chains that flow together under an imposed external stress, while interacting with neighboring groups of polymer chains (Fig. 4c).[35]

According to the model, increasing acrylamide concentration at a cross-linker ratio of 1 : 10 800 led to the significant increase in gel strength from 2540 ± 490 to 28 000 ± 6200 Pa (Fig. 4b–i). There was a minimal difference of the gel strength between the 9% w/w gel cross-linked at a ratio of 1 : 63 and the 29% w/w gel cross-linked at a ratio of 1 : 10 800. In contrast, the number of flow units was dropped dramatically as the cross-linker ratio was decreased from 1 : 63 to 1 : 10 800 (Fig. 4b-ii). At a cross-linker ratio of 1 : 10 800, the number of flow units was independent of the acrylamide concentration.

4. Analysis of various manipulations enabled by stretchable and tough gels.

The one-component stretchable and tough gels were evaluated for their ability to allow for various manipulations such as puncturing, suturing, and delivery using a syringe without being fractured or permanently deformed. First, the tough gel formed using 29% w/w acrylamide and a 1 : 10 800 cross-linker ratio was punctured with a needle without any crack propagation around the punctured area (Fig. 5a and Video S.1, S.2, ESI†). In contrast, the gel formed with 9% w/w acrylamide and a 1 : 63 cross-linker ratio allowed for crack propagation from the punctured location (Video S.3, ESI†).

A tough gel tube could be fabricated by forming a hydrogel with 29% w/w acrylamide solution and a cross-linking ratio of 1 : 10 800 within a 3-D printed cylindrical mold with various diameters (Scheme 1). The hollow gel tube could be sucked up into a syringe through a small aperture of 2 mm (more than half the diameter of the tube). The gel could be released from the syringe through the opening and recover the original shape

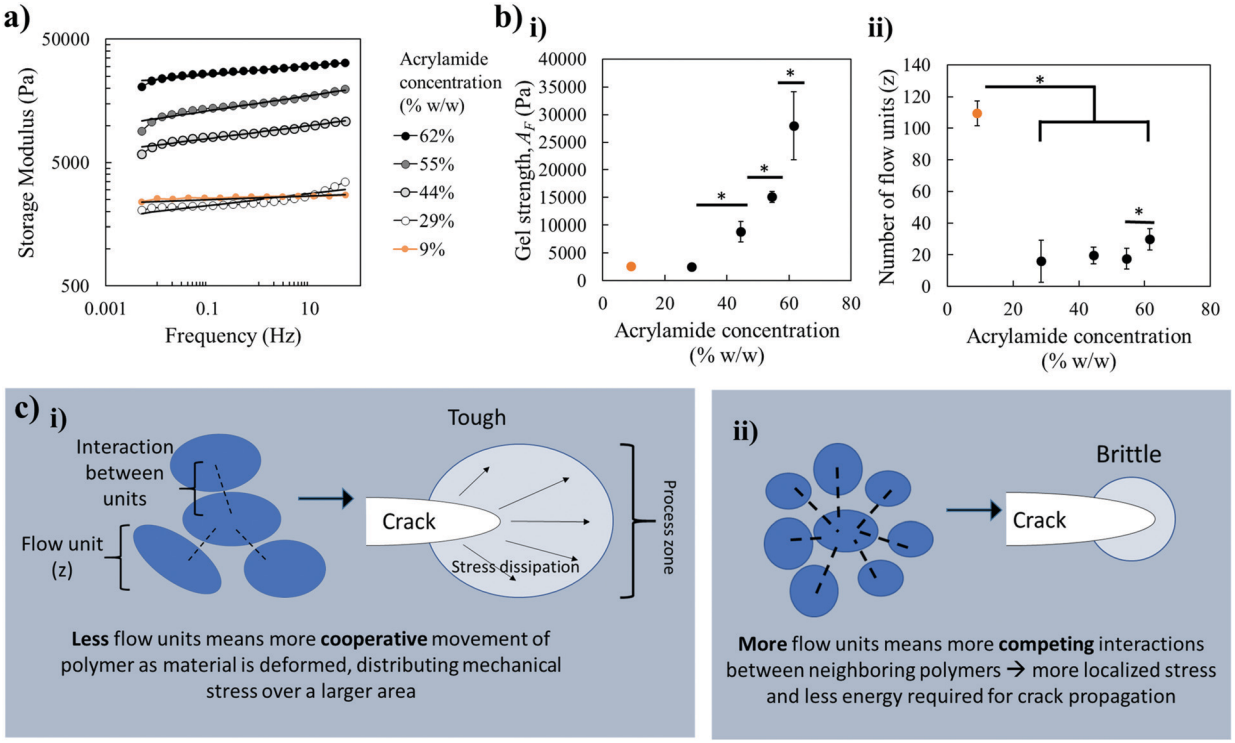

Fig. 4 Oscillatory shear rheology of hydrogels in response to frequency sweep The mechanical properties of hydrogels at various concentrations were measured under oscillatory shear using a rheometer over a range of oscillation frequencies. The data shown are (a) the shear storage modulus *vs.* frequency. The solid lines in the storage modulus *vs.* frequency graph are the values predicted by the Gabriele, De Cindio, and D'Antona gel model. (b) The gel model parameters that were fit to the oscillatory shear frequency sweep are plotted for the gels formed from various concentrations of acrylamide. The model parameters are (i) gel strength and (ii) the number of flow units. The values and error bars represent average and standard deviation of four different samples per condition. * indicates statistically significant difference in the means between samples according to a *T*-test with $p < 0.05$. (c) Schematic description of the fit parameter, z, flow units for (i) the tough hydrogels and (ii) the brittle hydrogel. Orange lines and points depict samples formed with a cross-linking ratio of 1 : 63. All other samples are formed with a cross-linking ratio of 1 : 10 800.

without any fracture or permanent deformation (Fig. 5b and Video S.4, ESI†).

In addition, the tough gel was formulated to present a similar elastic modulus of soft tissue such as 6 to 40 kPa, in order to fabricate gel-based tissue/organ mimics for suturing practice. The resulting gel did not show any crack propagation at sutured sites, while the brittle gel tube made with 9% acrylamide solution and cross-linker ratio of 1 : 63 easily fractures at the sutured site. The extent that the gel resists crack propagation at the sutured site was examined by pulling a single suture from a gel strip using a mechanical tester. As shown in Fig. 6a, b and Videos S.5–S.9 (ESI†), the tough gel formed using 29% w/w acrylamide and a 1 : 10 800 cross-linker ratio could even be stretched significantly by pulling on the suture. In contrast, the suture easily sliced through the brittle gel. All the tough hydrogels demonstrated at least a 20 times higher suture retention strength than the brittle hydrogel with 9% w/w acrylamide and a 1 : 63 molar cross-linker ratio (Fig. 6c).

Additionally, increasing acrylamide concentration at a cross-linker ratio of 1 : 108 000 increased the suture retention strength (Fig. 6d). This increase in suture retention strength allowed for two hydrogel pieces to be fully sutured together with many individual sutures and then stretched without crack formation (Video S.10, ESI†). We further fabricated the soft and tough gel into an artery-like form for microsurgical simulation that involves suturing of transected arteries in a surgical anastomosis procedure (Videos S.11–S.13, ESI†). Again, the tough gel tube could be anastomosed with sutures and also sustain sutured sites from external stress (Fig. 6e).

Discussion

These results have demonstrated that the toughness of the single-component polyacrylamide gel can be increased significantly by tuning the acrylamide concentration and cross-linking ratio (*i.e.*, mole of bis-acrylamide: mole of acrylamide). Specifically, increasing the acrylamide concentration from 9% w/w to 29% w/w and higher while tuning the cross-linker ratio from 1 : 63 to 1 : 10 800 produced a more than 30-fold increase of the energy to fracture. In addition, this strategy allowed for an increase an elastic modulus of the gel while maintaining a high energy to fracture around 1800 to 2600 J m^{-2}. The resulting tough gel could retain its structural integrity during penetration with needles and surgical suturing simulation.

In such hydrogels, rather than behaving purely elastically to an imposed strain, the polymer chains can dissipate more energy by flowing past one another. This additional potential

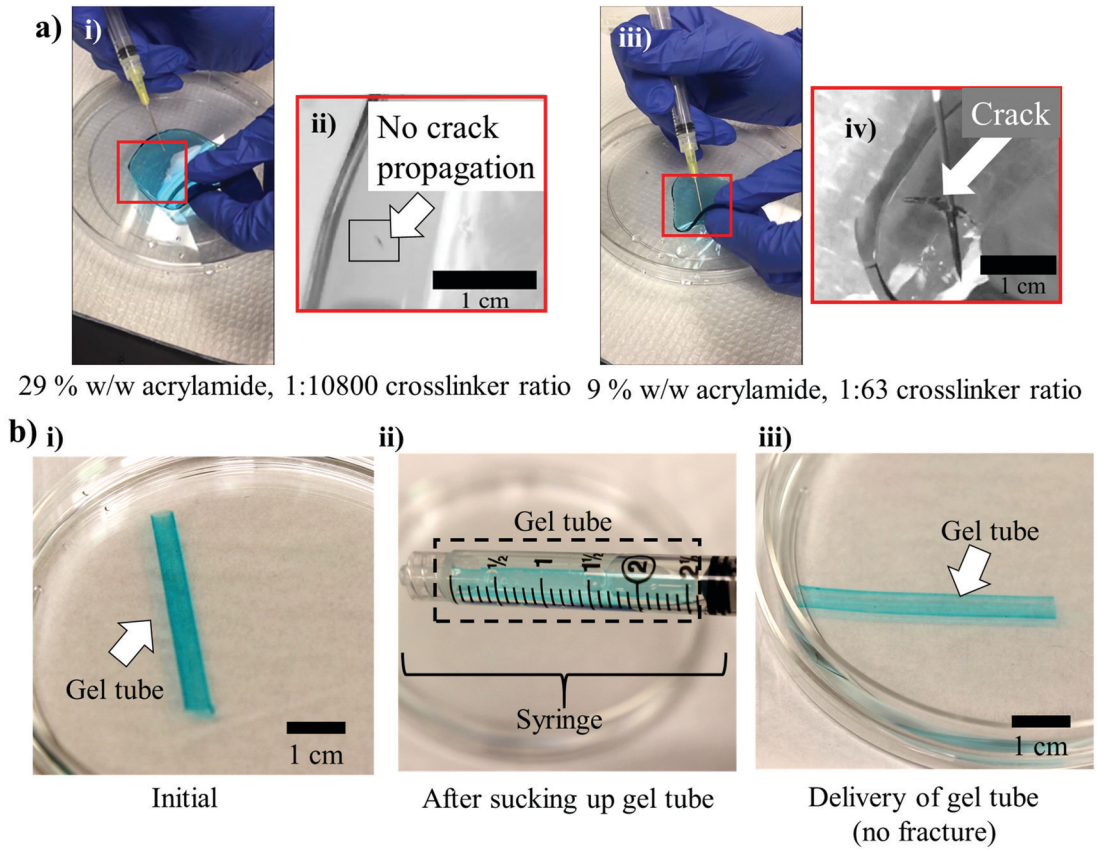

Fig. 5 Stretchable and tough hydrogels allowing for puncturing and syringe-based injection (a) The response of the hydrogels to puncture with a 22-gauge steel needle was photographed for the gels made with (i) and (ii) 29% w/w acrylamide and 1 : 10 800 cross-linking ratio and (iii) and (iv) 9% w/w acrylamide and 1 : 63 cross-linking ratio. (b) (i) Hydrogel tubes made with 29% w/w acrylamide and 1 : 10800 cross-linking were (ii) sucked up and (iii) delivered to a new location in solution using a syringe to demonstrate that fracture did not occur despite the large deformation.

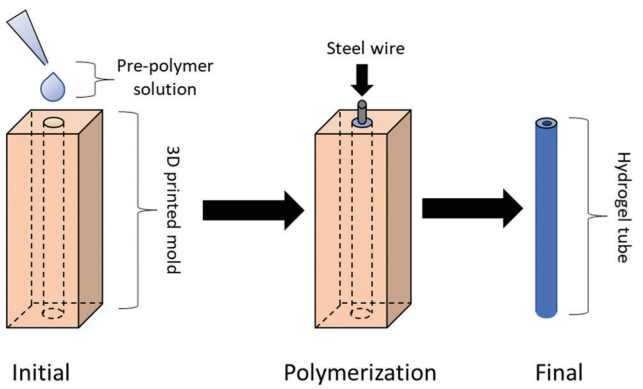

Scheme 1 Fabrication of tough, blood-vessel mimicking hydrogel tube using 3D printed mold.

for the gels to dissipate energy leads to an overall increase in fracture energy. The extent that the gel dissipates energy was also shown with the loss factor (*i.e.*, the ratio of loss to elastic modulus) quantified using oscillatory shear rheological experiments. The tough gels formed with a cross-linker ratio of 1 : 10 800 showed loss factors lying around 0.1. This value is from 2 to 7-fold higher than the loss factor of the brittle 9% w/w hydrogel with the cross-linker ratio of 1 : 63 depending on the frequency from 0.005 to 50 Hz. Commonly, loss factors above 0.1 are found in dissipative, physical gels.[36,37]

The dependence of shear modulus on the frequency characterized with the oscillatory shear measurement is also characteristic of energy dissipation.[38] This dependence was characterized using a "flow unit" model, revealing a number of "flow units" interactions per polymer chain.[32] The flow unit represents a group of polymer chains that flow together under an imposed external stress, while interacting with neighboring groups of polymer chains.[35] The area where individual flow units interact stores and accumulates stress during deformation. Therefore, the ability of the gel to dissipate energy is inversely related to the number of flow units. According the analysis of the rheological data using eqn (4), the tough and stretchable hydrogels showed more than five times fewer flow units compared to the brittle, 9% w/w acrylamide hydrogel with the cross-linker ratio of 1 : 63. This decrease could indicate that polymer chains in the tough gel dissipate energy as larger units than the those in the brittle gel (*i.e.*, 9% w/w gel with a 1 : 63 cross-linker ratio), as the gels are deformed. In addition, the 9% w/w gel with a 1 : 63 cross-linker ratio has more covalent bonds per polymer chain than the hydrogels with a 1 : 10 800 cross-linker ratio, which also leads to increased stress concentration and fracture at an earlier strain.

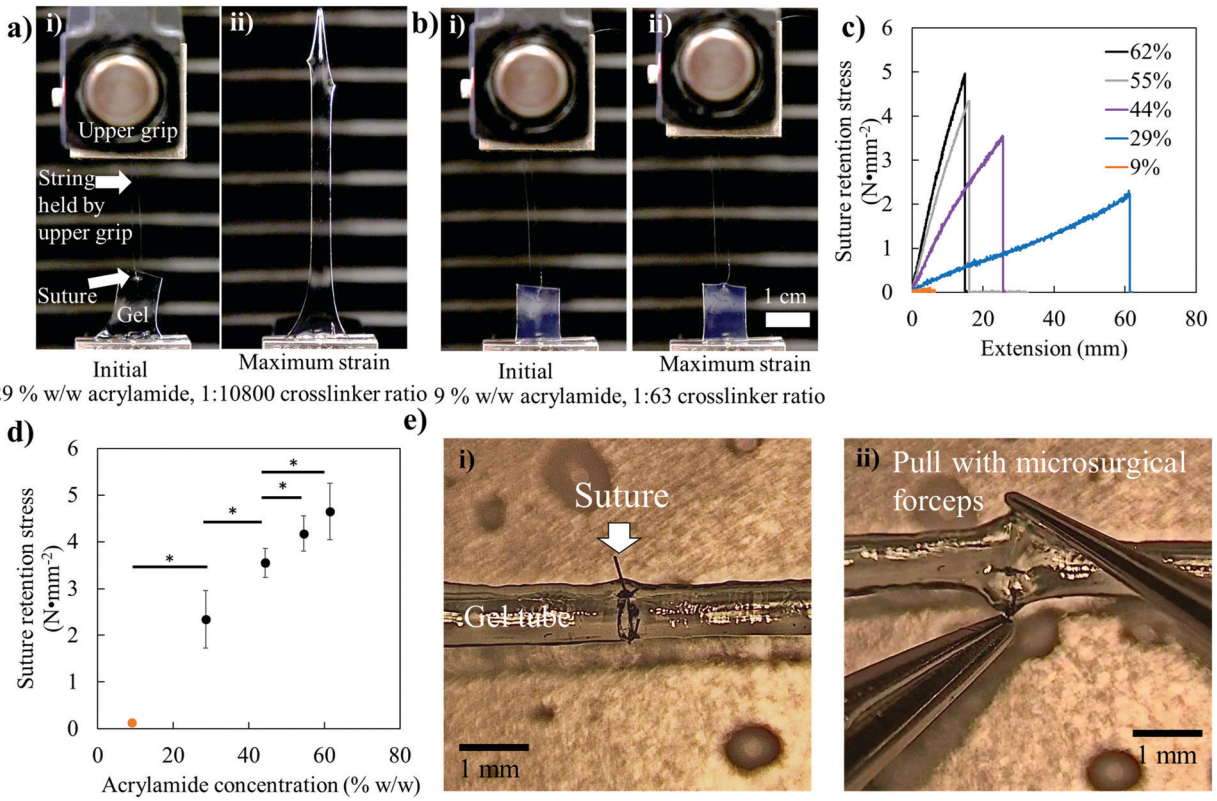

Fig. 6 Stretchable and tough hydrogels allowing for suturing and simulated vascular surgery Hydrogels made with (a) 29% w/w acrylamide and 1 : 10 800 cross-linking ratio and (b) 9% w/w acrylamide and 1 : 63 cross-linking ratio were sutured on one end and gripped by the mechanical tensile tester on the other. The string of the sutured end was clamped by the upper grip of the mechanical tester. Photos of the gels made taken using the same gel compositions as the puncture test both (i) initially and (ii) just before fracture. (c) Representative suture retention strength *vs.* extension curves obtained for sutured gels under uniaxial tensile extension. The retention strength was calculated by dividing the measured load by the product of the gel thickness and suture string diameter. (d) The maximum observed suture retention strength before fracture for hydrogels with various acrylamide concentrations. The values and error bars represent average and standard deviation of at least five different samples per condition. * indicates statistically significant difference in the means between samples according to a *T*-test with $p < 0.05$. (e) A 1 mm diameter gel tube was formed with 29% w/w acrylamide and 1 : 10 800 cross-linking ratio was cut, clamped into position, then sutured to simulate microvascular surgery. The gel tube could be sutured together and the sutures could be pulled on without crack formation. Orange points and lines depict samples formed with a cross-linking ratio of 1 : 63. All other samples are formed with a cross-linking ratio of 1 : 10 800.

Despite these multiple indicators of a dissipative polymeric network, the dependence of the elastic modulus on acrylamide concentration revealed that the tough hydrogels behave as a viscoelastic network. For example, the dependence of the plateau storage modulus on concentration is a ~1.8 power dependence, which is intermediately between 2.2 predicted for cross-linked polymers with a smaller mesh size than the persistence length and 1.4 which is predicted for an entangled polymer solution (Fig. S.8, ESI†).[39,40] Therefore, we propose that the hydrogels with a cross-linker ratio of 1 : 10 800 behave with intermediate properties between a purely elastic gel and an entangled polymer solution.

The storage modulus and concentration are related by the scaling relationship Eqn 2:[41]

$$G \approx G'' \quad (2)$$

where G is the shear storage modulus and C is the acrylamide concentration. Using the relation between concentration and polymer screening length, the dependency of G and C can be further modified to relate to the fractal dimension between junctions, $1/\nu$, by using eqn (3):[42,43]

$$G \approx C^{3\nu/(3\nu-1)} \quad (3)$$

The fractal dimensionality indicates the interaction of the polymer with the surrounding solvent, and therefore offers insight into the conformation of the polymer, where $1/\nu = 2$ for a polymer in a theta solvent and greater than 2 for a solvent poorer than a theta solvent.[44] The shear storage modulus was defined as the plateau modulus in the frequency domain when the loss factor was at a minimum according to Fig. 4a and Fig. S.8 (ESI†). Using the exponent dependency between the elastic modulus and acrylamide concentration, $1/\nu$ was calculated to be greater than or equal to 2. This value indicates that the tough hydrogels with a cross-linker ratio of 1 : 10 800 consist of a polymer network that exists within a nearly theta solvent and therefore adopts the conformation of an ideal chain described by a random walk coil.[45] Thus, the tough gels resemble a chemically cross-linked gel rather than a physical

gel. As a consequence, the elasticity of the tough hydrogels allows the gels to recover their original shape after large deformations such as syringe-based injection.

In addition, the dependence of the fracture behavior on strain rate supports the presence of a heavily entangled polymeric network in the tough hydrogels. As the strain rate increases, both the ultimate tensile strain and energy to fracture decrease. As the strain rate increases, it is likely that the polymer chains are given less time to reorient themselves to decrease the chain free energy. Therefore, at higher strain rates, there are more interactions between chains that can act as focal points of stress.

Informed by these results, we suggest that the single-component tough gel could be assembled by increasing entanglements of polymer chains between covalently cross-linked junctions. This gel would give rise to the same two elements that make up the toughening mechanism shown by other binary tough and stretchable hydrogels: (1) short-range non-covalent interactions that give rise to viscous properties and, in turn, energy dissipative mechanisms and (2) long-range, covalent bonds that provides elastic properties to restore its original shape reversibly following a large deformation.[40,46] This proposed gel microstructure can help to explain the increase in the maximum tensile strain and energy dissipation of the hydrogels with a molar cross-linker ratio of 1 : 10 800, since these gels have a decreased length of polymer between cross-links. The length of polymer between cross-links inversely proportional to the number of effective cross-links per volume ($N_{\text{cross-link}}$).

Altogether, the significant energy dissipation process within the tough hydrogels allows them to withstand much higher loads from a suture compared to the brittle hydrogel. This mechanism allows us to tune an elastic modulus of the gel with minimal change of the toughness, such that the gel can reproduce softness and crack growth resistance of target organs. Such suture-resistant hydrogels would be useful for several applications, such as preoperative surgery planning, simulation, and training, since they can withstand shear forces while providing tissue-like softness and hydration. This material tool would be invaluable for surgeons to develop the most efficacious surgical strategy and also acquire the precise dexterity, hand-eye coordination, and motor skills necessary for veterinary and human surgery, microsurgery, and minimally invasive surgery.[2] Having an accurate non-animal model on which to perform simulation exercises would facilitate the transfer of such skills to real life surgical contexts. We also suggest single-component, tough and stretchable hydrogels could be formed by numerous other polymeric hydrogel systems by forming gels with orchestrated control of non-ionic monomer concentration and cross-linking ratio. This could be achieved in polymers that have both high solubility and the potential to form entanglements between chains.

Experimental methods

Polyacrylamide hydrogel synthesis

Stretchable and tough polyacrylamide hydrogels were prepared by varying acrylamide monomer concentration (29, 44, 55, and 62% acrylamide w/w total) and a 1 : 10 800 molar ratio of methylene bis-acrylamide to acrylamide (cross-linking ratio). Acrylamide concentrations above 40% w/w were fully dissolved by briefly heating the solution using a 37 °C warm water bath. A polyacrylamide hydrogel of 10% monomer concentration and a 1 : 63 cross-linking ratio was also prepared to prepare a brittle polyacrylamide hydrogel.[47] The gels were synthesized by mixing appropriate amounts (*i.e.*, according to the intended weight fraction and cross-linking ratios) of solid acrylamide and methylene bis-acrylamide into deionized water. Then, 10 μL of 10% w/v ammonium persulfate and 2 μL tetramethylethylene diamine were mixed into 1 mL of the monomer/cross-linker solution. After mixing, the resulting solution was poured in between glass plates with a 1 mm spacer. After allowing 30 minutes to polymerize, each gel was allowed to swell in water for at least twelve hours.

Polymer volume fraction and number of cross-links measurement

Hydrogels were prepared as previously described and cut into disks of 2 cm diameter. After swelling in water, the individual gels were weighed to obtain the swollen weight of the hydrogels. Once the swollen weights were obtained, the gels were then frozen for at least twelve hours and subsequently dried using a lyophilizer. The dried hydrogels were then weighed to obtain the dried weights. The volume fraction of polymer in the equilibrium swollen gel (v_p) was then calculated with the following eqn (4):[10]

$$\frac{1}{v_p} = \rho_p\left(\frac{Q_m}{\rho_s} + \frac{1}{\rho_p}\right) \tag{4}$$

where ρ_s is the density of water, ρ_p is the density of polymer (1.386 g cm^{-3}), Q_m is the swelling ratio (*i.e.*, mass ratio of swollen to dried gel). The measured shear modulus and the polymer volume fraction (v_p) were then used to quantify the number of elastically effective cross-links per unit volume ($N_{\text{cross-link}}$) using a rubber elasticity model that has been modified to account for the proportion of water within the hydrogel (eqn (5)):[10,26,48–50]

$$N_{\text{cross-link}} = \frac{G v_p^{-1/3}}{RT} \tag{5}$$

where G is the shear modulus of the gel, R is the ideal gas constant, and T is the temperature that the measurements were taken (298 K).[51] G was calculated from hydrogels in the equilibrium swelling condition using the complex modulus G^* measured when G'' was at a minimum in the rheological frequency sweep.

Tensile mechanical tests

Following swelling of the gels in water until equilibrium, one rectangular strip of width 1 cm was cut *via* razor blade. To make notched samples, a razor blade was used to cut notches of length 0 mm, 3 mm, and 6 mm on one side of the strip. Each gel strip was mounted on a mechanical tensile tester (MTS Insight 1) with an initial gage distance of 5 mm and elongated until fracture at a constant strain rate (either 0.01, 0.1, or 1 s^{-1}).

During the slow tensile tests at 0.01 s^{-1}, the gels were kept hydrated during the test using a water mist generator. Using this data, the total work absorbed by the gel until fracture (W_{total}) was quantified with sum of the work dissipated within the fracture process zone (W_p) and the work dissipated outside the fracture process zone (W_0) as shown in eqn (6):[29]

$$W_{total} = W_p + W_0 \quad (6)$$

For notched specimens, eqn (6) was normalized by the initial cross-sectional area of the gel between the notches to obtain eqn (7):

$$w_{total} = w_p + blw_o \quad (7)$$

In this way, the essential work (w_{total}) was related to the essential work dissipated within the fracture process zone (w_p), and the essential work dissipated outside the fracture process zone (w_0), while b is a shape factor (1.5 for a linear slit notch) and l is the initial distance between the notches. w_{total} is the energy to fracture displayed in Fig. 2b and w_p and w_0 are calculated using a linear regression. The normalized dissipated work displayed in Fig. 2c is w_0 for a given sampled divided by w_0 for the hydrogel made with 9% w/w acrylamide and a 1 : 63 molar cross-linker ratio.

The presence of strain hardening in the gel samples was evaluated from the abovementioned tensile testing data. First, the measured stress (σ) and strain (γ) were converted into true stress (σ_{true}) and elongation parameter ($\lambda^2 - 1/\lambda$) *via* the following eqn (8) and (9) that normalizes the stress by the instantaneous cross-sectional area assuming that the material is incompressible:

$$\sigma_{true} = \sigma(1 + \gamma) \quad (8)$$

$$\lambda = 1 + \gamma \quad (9)$$

Then, the resulting true stress *vs.* elongation factor curves were plotted. Deviation from linearity of these curves indicates strain hardening. In contrast, a linear response indicates that the mechanical response is largely elastic with minimal strain hardening.

Suture tensile tests were also performed using gel strips of width 1 cm. For each sample, a suture needle (Ethicon, 16 mm length, 1/2 circle) was inserted 2 mm from the edge of the sample in the center. The thread used was 0.1 mm nylon (5-0). The sample was then carefully placed on the tensile testing machine with the material clamped with the bottom grip and the suture string fastened to the top grip, with 1 cm of material in between the grips. The sample was elongated to fracture at a rate of 1 cm min^{-1}. Suture retention strength was calculated using the following eqn (10):[52]

$$\text{Suture retention strength} = \frac{\text{Maximum load}}{\text{Sample thickness} \times \text{Suture string diameter}} \quad (10)$$

Shear rheology frequency sweep

Hydrogels were prepared as previously mentioned and cut into 1.5 cm diameter disks. These gels were and loaded onto a rheometer (TA Instruments, DHR-3) in parallel plate geometry with a diameter of 1.5 cm. During each experiment, the chamber was closed and sealed with damp tissues to minimize water evaporation. Before each frequency sweep, an amplitude sweep from 0.001 to 1% strain was performed at a frequency of 1 Hz to ensure that the tests were performed in the linear regime. The frequency sweeps from 0.005 to 50 Hz were performed with an oscillation amplitude of 0.1% strain.

Conclusion

Overall, this study demonstrates a simple but unique strategy to assemble a single-component, stretchable and tough hydrogel with controlled tissue-like softness using a polyacrylamide hydrogel with increased acrylamide concentration and distant cross-links. This mechanical property was attained from dense entanglements between gel-forming polymers that serve to dissipate energy by flowing rather than localizing stress at covalent cross-links. This mechanism was confirmed by analyzing the response of the material to both tensile fracture and shear rheology. In particular, tensile tests revealed a large amount of work dissipated outside of the fracture zone. Shear rheology also revealed that the tough hydrogels exhibited a decrease in the number of flow units, indicating more cooperative movement of polymer bundles and an increase in area of the fracture process zone. The resulting stretchable and tough gel allowed for various manipulations including puncturing, suturing, and syringe-based injection used during surgery and less invasive implant/device delivery. We envisage that the results of this study can be broadly applied to improving controllability of other gel properties. Since only one polymer component is required for this synthesis, doing so would greatly simplify the fabrication of stretchable and tough hydrogels.

Conflicts of interest

There are no conflicts of interest to declare.

Acknowledgements

This work was supported by the National Science Foundation (STC-EBICS Grant CBET-0939511 to HJK) and TechnipFMC (IL Reference #093250 to W. C. B.). This project has been funded by the Jump ARCHES endowment through the Health Care Engineering Systems Center at University of Illinois at Urbana-Champaign. YH would like to acknowledge the funding support from the National Science Foundation under Grant No. 1554326 and the US Air Force Office of Scientific Research Multidisciplinary University Research Initiative under Award FA9550-09-1-0669-DOD35CAP. Simon Rogers at UIUC for rheometer usage.

References

1 W. Su, Y. Xiao, S. He, P. Huang and X. Deng, Three-dimensional printing models in congenital heart disease education for medical students: A controlled comparative

study, *BMC Med. Educ.*, 2018, **18**, 178, DOI: 10.1186/s12909-018-1293-0.

2 A. Ganguli, G. J. Pagan-Diaz, L. Grant, C. Cvetkovic, M. Bramlet, J. Vozenilek, T. Kesavadas and R. Bashir, 3D printing for preoperative planning and surgical training: a review, *Biomed. Microdevices*, 2018, **20**, 1–24, DOI: 10.1007/s10544-018-0301-9.

3 R. Sodian, D. Schmauss, M. Markert, S. Weber, K. Nikolaou, S. Haeberle, F. Vogt, C. Vicol, T. Lueth, B. Reichart and C. Schmitz, Three-Dimensional Printing Creates Models for Surgical Planning of Aortic Valve Replacement After Previous Coronary Bypass Grafting, *Ann. Thorac. Surg.*, 2008, **85**, 2105–2108, DOI: 10.1016/j.athoracsur.2007.12.033.

4 B. Fletcher, J. De La Ree and J. Drougas, Development of a pulsatile, tissue-based, versatile vascular surgery simulation laboratory for resident training, *J. Vasc. Surg. Cases Innov. Tech.*, 2017, **3**, 209–213, DOI: 10.1016/j.jvscit.2017.06.003.

5 C. He, S. W. Kim and D. S. Lee, In situ gelling stimuli-sensitive block copolymer hydrogels for drug delivery, *J. Controlled Release*, 2008, **127**, 189–207, DOI: 10.1016/j.jconrel.2008.01.005.

6 Y. Chen, X. H. Pang and C. M. Dong, Dual stimuli-responsive supramolecular polypeptidebased hydrogel and reverse micellar hydrogel mediated by host-guest chemistry, *Adv. Funct. Mater.*, 2010, **20**, 579–586, DOI: 10.1002/adfm.200901400.

7 S. Q. Liu, C. Yang, Y. Huang, X. Ding, Y. Li, W. M. Fan, J. L. Hedrick and Y. Y. Yang, Antimicrobial and antifouling hydrogels formed in situ from polycarbonate and poly(ethylene glycol) via Michael addition, *Adv. Mater.*, 2012, **24**, 6484–6489, DOI: 10.1002/adma.201202225.

8 K. Ariga, K. Kawakami and J. P. Hill, Emerging pressure-release materials for drug delivery, *Expert Opin. Drug Delivery*, 2013, **10**, 1465–1469, DOI: 10.1517/17425247.2013.819340.

9 X. Zhao, Multi-scale multi-mechanism design of tough hydrogels: Building dissipation into stretchy networks, *Soft Matter*, 2014, **10**, 672–687, DOI: 10.1039/c3sm52272e.

10 H. J. Kong, E. Wong and D. J. Mooney, Independent control of rigidity and toughness of polymeric hydrogels, *Macromolecules*, 2003, **36**, 4582–4588, DOI: 10.1021/ma034137w.

11 M. S. Shoichet, R. H. Li, M. L. White and S. R. Winn, Stability of hydrogels used in cell encapsulation: An in vitro comparison of alginate and agarose, *Biotechnol. Bioeng.*, 1996, **50**, 374–381, DOI: 10.1002/(SICI)1097-0290(19960520)50:4 < 374::AID-BIT4 > 3.0.CO;2-I.

12 W. Wang, Y. Zhang and W. Liu, Bioinspired fabrication of high strength hydrogels from non-covalent interactions, *Prog. Polym. Sci.*, 2017, **71**, 1–25, DOI: 10.1016/j.progpolymsci.2017.04.001.

13 J. P. Gong, Why are double network hydrogels so tough?, *Soft Matter*, 2010, **6**, 2583, DOI: 10.1039/b924290b.

14 J. Y. Sun, X. Zhao, W. R. K. Illeperuma, O. Chaudhuri, K. H. Oh, D. J. Mooney, J. J. Vlassak and Z. Suo, Highly stretchable and tough hydrogels, *Nature*, 2012, **489**, 133–136, DOI: 10.1038/nature11409.

15 K. Ito, Novel cross-linking concept of polymer network: Synthesis, structure, and properties of slide-ring gels with freely movable junctions, *Polym. J.*, 2007, **39**, 489–499, DOI: 10.1295/polymj.PJ2006239.

16 Y. Okumura and K. Ito, The polyrotaxane gel: A topological gel by figure-of-eight cross-links, *Adv. Mater.*, 2001, **13**, 485–487, DOI: 10.1002/1521-4095(200104)13:7 < 485::AID-ADMA485 > 3.0.CO;2-T.

17 M. Kobayashi, Y. S. Chang and M. Oka, A two year *in vivo* study of polyvinyl alcohol-hydrogel (PVA-H) artificial meniscus, *Biomaterials*, 2005, **26**, 3243–3248, DOI: 10.1016/j.biomaterials.2004.08.028.

18 Y. Li, Y. Sun, Y. Xiao, G. Gao, S. Liu, J. Zhang and J. Fu, Electric Field Actuation of Tough Electroactive Hydrogels Cross-Linked by Functional Triblock Copolymer Micelles, *ACS Appl. Mater. Interfaces*, 2016, **8**, 26326–26331, DOI: 10.1021/acsami.6b08841.

19 L. Han, X. Lu, M. Wang, D. Gan, W. Deng, K. Wang, L. Fang, K. Liu, C. W. Chan, Y. Tang, L. T. Weng, H. Yuan and A. Mussel-Inspired, Conductive, Self-Adhesive, and Self-Healable Tough Hydrogel as Cell Stimulators and Implantable Bioelectronics, *Small*, 2017, **13**, 1601916, DOI: 10.1002/smll.201601916.

20 T. Kakuta, Y. Takashima and A. Harada, Highly elastic supramolecular hydrogels using host-guest inclusion complexes with cyclodextrins, *Macromolecules*, 2013, **46**, 4575–4579, DOI: 10.1021/ma400695p.

21 J. Hao and R. A. Weiss, Mechanical behavior of hybrid hydrogels composed of a physical and a chemical network, *Polymer*, 2013, **54**, 2174–2182, DOI: 10.1016/j.polymer.2013.01.052.

22 D. C. Tuncaboylu, M. Sari, W. Oppermann and O. Okay, Tough and self-healing hydrogels formed via hydrophobic interactions, *Macromolecules*, 2011, **44**, 4997–5005, DOI: 10.1021/ma200579v.

23 S. Z. Mao, X. D. Zhang, J. M. Dereppe and Y. R. Du, Nuclear magnetic resonance relaxation studies of polyacrylamide solution, *Colloid Polym. Sci.*, 2000, **278**, 264–269, DOI: 10.1007/s003960050042.

24 Y. Hagiwara, A. Putra, A. Kakugo, H. Furukawa and J. P. Gong, Ligament-like tough double-network hydrogel based on bacterial cellulose, *Cellulose*, 2010, **17**, 93–101, DOI: 10.1007/s10570-009-9357-2.

25 Y. Wang, J. Wu, Z. Cao, C. Ma, Q. Tong, J. Li, H. Liu, J. Zheng and G. Huang, Mechanically robust, notch-insensitive, fatigue resistant and self-recoverable hydrogels with homogeneous and viscoelastic network constructed by a novel multifunctional cross-linker, *Polymer*, 2019, **179**, 121661, DOI: 10.1016/j.polymer.2019.121661.

26 K. S. Anseth, C. N. Bowman and L. Brannon-Peppas, Mechanical properties of hydrogels and their experimental determination, *Biomaterials*, 1996, **17**, 1647–1657, DOI: 10.1016/0142-9612(96)87644-7.

27 F. Luo, T. L. Sun, T. Nakajima, T. Kurokawa, Y. Zhao, A. Bin Ihsan, H. L. Guo, X. F. Li and J. P. Gong, Crack blunting and advancing behaviors of tough and self-healing polyampholyte hydrogel, *Macromolecules*, 2014, **47**, 6037–6046, DOI: 10.1021/ma5009447.

28 J. Ma, J. Lee, S. S. Han, K. H. Oh, K. T. Nam and J. Y. Sun, Highly Stretchable and Notch-Insensitive Hydrogel Based

on Polyacrylamide and Milk Protein, *ACS Appl. Mater. Interfaces*, 2016, **8**, 29220–29226, DOI: 10.1021/acsami.6b10912.

29 B. Cotterell and J. K. Reddel, The essential work of plane stress ductile fracture, *Int. J. Fract.*, 1977, **13**, 267–277, DOI: 10.1007/BF00040143.

30 J. Lee, C. W. Macosko and D. W. Urry, Mechanical properties of cross-linked synthetic elastomeric polypentapeptides, *Macromolecules*, 2001, **34**, 5968–5974, DOI: 10.1021/ma0017844.

31 R. N. Haward, The derivation of a strain hardening modulus from true stress-strain curves for thermoplastics, *Polymer*, 1994, **35**, 3858–3862, DOI: 10.1016/0032-3861(94)90268-2.

32 H. H. Winter, Can the gel point of a cross-linking polymer be detected by the $G' - G''$ crossover?, *Polym. Eng. Sci.*, 1987, **27**, 1698–1702, DOI: 10.1002/pen.760272209.

33 A. Martínez-Ruvalcaba, E. Chornet and D. Rodrigue, Viscoelastic properties of dispersed chitosan/xanthan hydrogels, *Carbohydr. Polym.*, 2007, **67**, 586–595, DOI: 10.1016/j.carbpol.2006.06.033.

34 D. Gabriele, B. De Cindio and P. D'Antona, A weak gel model for foods, *Rheol. Acta*, 2001, **40**, 120–127, DOI: 10.1007/s003970000139.

35 L. Bohlin, A theory of flow as a cooperative phenomenon, *J. Colloid Interface Sci.*, 1980, **74**, 423–434, DOI: 10.1016/0021-9797(80)90211-8.

36 S. Abdurrahmanoglu, V. Can and O. Okay, Design of high-toughness polyacrylamide hydrogels by hydrophobic modification, *Polymer*, 2009, **50**, 5449–5455, DOI: 10.1016/j.polymer.2009.09.042.

37 S. B. Ross-Murphy, Structure–property relationships in food biopolymer gels and solutions, *J. Rheol.*, 1995, **39**, 1451–1463, DOI: 10.1122/1.550610.

38 D. T. N. Chen, Q. Wen, P. A. Janmey, J. C. Crocker and A. G. Yodh, Rheology of Soft Materials, *Annu. Rev. Condens. Matter Phys.*, 2010, **1**, 301–322, DOI: 10.1146/annurev-conmatphys-070909-104120.

39 B. Hinner, M. Tempel, E. Sackmann, K. Kroy and E. Frey, Entanglement, elasticity, and viscous relaxation of actin solutions, *Phys. Rev. Lett.*, 1998, **81**, 2614–2617, DOI: 10.1103/PhysRevLett.81.2614.

40 F. C. MacKintosh, J. Käs and P. A. Janmey, Elasticity of semiflexible biopolymer networks, *Phys. Rev. Lett.*, 1995, **75**, 4425–4428, DOI: 10.1103/PhysRevLett.75.4425.

41 P.-G. de Gennes, Scaling Concepts in Polymer Physics, 1979.

42 R. Hernández, A. Sarafian, D. López and C. Mijangos, Viscoelastic properties of poly(vinyl alcohol) hydrogels and ferrogels obtained through freezing-thawing cycles, *Polymer*, 2004, **45**, 5543–5549, DOI: 10.1016/j.polymer.2004.05.061.

43 M. Daoud, J. P. Cotton, B. Farnoux, G. Jannink, G. Sarma, H. Benoit, C. Duplessix, C. Picot and P. G. de Gennes, Solutions of Flexible Polymers. Neutron Experiments and Interpretation, *Macromolecules*, 1975, **8**, 804–818, DOI: 10.1021/ma60048a024.

44 S. Havlin and D. Ben-Avraham, Fractal dimensionality of polymer chains, *J. Phys. A: Math. Gen.*, 1982, **15**, 6, DOI: 10.1088/0305-4470/15/6/011.

45 H. E. Stanley, Application of fractal concepts to polymer statistics and to anomalous transport in randomly porous media, *J. Stat. Phys.*, 1984, **36**, 843–860, DOI: 10.1007/BF01012944.

46 D. Myung, W. Koh, J. Ko, Y. Hu, M. Carrasco, J. Noolandi, C. N. Ta and C. W. Frank, Biomimetic strain hardening in interpenetrating polymer network hydrogels, *Polymer*, 2007, **48**, 5376–5387, DOI: 10.1016/j.polymer.2007.06.070.

47 A. Chrambach and D. Rodbard, Polyacrylamide gel electrophoresis, *Science*, 1971, **172**, 440–451.

48 P. J. Flory, N. Rabjohn and M. C. Shaffer, Dependence of elastic properties of vulcanized rubber on the degree of cross linking, *J. Polym. Sci.*, 1949, **4**, 225–245, DOI: 10.1002/pol.1949.120040301.

49 N. A. Peppas and E. W. Merrill, Crosslinked poly(vinyl alcohol) hydrogels as swollen elastic networks, *J. Appl. Polym. Sci.*, 1977, **21**, 1763–1770, DOI: 10.1002/app.1977.070210704.

50 L. R. G. Treloar, Elasticity and Related Properties of Rubbers, *Rubber Chem. Technol.*, 1974, **47**, 625–696, DOI: 10.5254/1.3540456.

51 Y. H. Bae, T. Okano and S. W. Kim, Temperature dependence of swelling of crosslinked poly(*N*,*N*′-alkyl substituted acrylamides) in water, *J. Polym. Sci., Part B: Polym. Phys.*, 1990, **28**, 923–936, DOI: 10.1002/polb.1990.090280609.

52 E. M. Jeffries, R. A. Allen, J. Gao, M. Pesce and Y. Wang, Highly elastic and suturable electrospun poly(glycerol sebacate) fibrous scaffolds, *Acta Biomater.*, 2015, **18**, 30–39, DOI: 10.1016/j.actbio.2015.02.005.

